Molecular modelling, Synthesis and Antiproliferative Evaluation of New Phenyldiazenyl)-Pyrazol Schiff Base Derivatives

Duha E. Taha*, Monther F. Mahdi and*, Ayad M. R. Raauf**

Department of Pharmaceutical Chemistry, College of Pharmacy, Mustansiriyah University, Baghdad, Iraq.

****College of Pharmacy, Al-Farahidi University, Baghdad, Iraq.***

Article Info:

Received Mar 2023
Revised May 2023
Accepted Jun 2023
Corresponding Author email:
dr.monther.f71@uomustansiriyah.edu.iq
Orcid: https://orcid.org/0000-0002-2069-4121

DOI: https://doi.org/10.32947/ajps.v24i1.999

Abstract:

Lung cancer is the most prevalent worldwide. In addition, it is also the most common cause of cancer-related deaths worldwide, with around 1.8 million new cases annually. With a 5-year survival rate of fewer than 20%. Cytotoxic medicines are commonly employed in cancer treatment. Although the medicine improves patients' quality of life, several disadvantages diminish its efficacy. This necessitates developing new effective strategies that target tumors with minimal adverse effects. This research aims to overcome these issues by synthesizing a new series of phenyldiazenyl)-pyrazol schiff base derivatives by utilizing the molecular docking (GOLD) suite program and the pharmacokinetic properties determination by utilizing (Swiss) ADME suite; The most appropriate-fitting compounds were subsequently produced and confirmed using spectrum analysis (FTIR, ^{1}HNMR, and ^{13} CNMR). MTT *in vitro* assay were performed to assess of antiproliferative activities against A549 lung cancer cell lines. The antiproliferative study showed that compound 3a had an inhibitory concentration (IC_{50} of 17.37 µM) on lung cancer cells (A549), which was significantly higher inhibitory activity than Erlotinib (IC_{50} = 25.06 µM). While compound 3b had an inhibitory activity comparable to the reference drug's, The IC_{50} values for compounds 3c, 3d, and 3e were 47.48, 45.56, and 33.05 µM, respectively.

Keywords: lung cancer, EGFR receptor, A549, molecular docking, pharmacokinetic study, pyrazole.

النمذجة الجزيئية والتوليف وتقييم مضاد التكاثر لمشتقات شف بيس فنيل ديازينيل بايروزول الجديدة

ضحى عماد طه*، منذر فيصل مهدي*، اياد محمد رشيد**

***قسم الكيمياء الصيدلانية، كلية الصيدلة، الجامعة المستنصرية، بغداد، العراق.*

****كلية الصيدلة، جامعة الفراهيدي، بغداد، العراق.*

الخلاصة

سرطان الرئة هو الأكثر انتشارًا في جميع أنحاء العالم. بالإضافة إلى ذلك ، فهو أيضًا السبب الأكثر شيوعًا للوفيات المرتبطة بالسرطان في جميع أنحاء العالم ، مع حوالي 1.8 مليون حالة جديدة سنويًا. بمعدل بقاء 5 سنوات أقل من 20٪. تستخدم الأدوية السامة للخلايا بشكل شائع في علاج السرطان. على الرغم من أن الدواء يحسن نوعية حياة المرضى ، إلا أن العديد من العيوب تقلل من فعاليته. وهذا يستلزم تطوير استراتيجيات فعالة جديدة تستهدف الأورام بأقل آثار ضارة. يهدف هذا البحث إلى التغلب على هذه المشكلات من خلال تخليق سلسلة جديدة من مشتقات شف بيس فنيل ديازينيل بايروزول الجديدة وبناءًا على الالتحام الجزيئي ببرنامج (GOLD) وتحديد الخصائص الحركية للدواء

باستخدام (SWISS ADME) ؛ ثم بعد ذلك تصنيع المركبات الأكثر ملاءمة وتأكيدها عن طريق التحليل الطيفي (FTIR, ^{1}HNMR ، ^{13}CNMR) ثم اجراء اختبار MTT في المختبر لتقييم الأنشطة المضادة للتكاثر ضد سلالات خلايا سرطان الرئة A549 أظهرت الدراسة المضادة للتكاثر أن المركب (3 أ)يحتوي على تركيز مثبط IC_{50} يبلغ 17.37 مايكرومولر على خلايا سرطان الرئة (A549) وهو نشاط مثبط أعلى بكثير من Erlotinib حيث يبلغ تركيزه المثبط IC_{50}=25,06 مايكرومولر بينما كان للمركب (3 ب) نشاط مثبط مشابه للعقار المرجعي ، كانت قيم IC_{50} للمركبات 3س , 3 د , 3ي هي 48.47 و 56.45 و 33.05 مايكرومولر على التوالي.

الكلمات الأساسية:

INTRODUCTION

Cancer has been identified as one of the most common causes of death worldwide because of its extensive and complex aetiology [1]. Cancer is a fatal disease, particularly in advanced countries. The mortality rate will rise to 13.1 million deaths in 2030 [2]. Tyrosine kinase receptors(TKRs) involve over 60 particles that play a crucial part in the molecular pathways that lead to differentiation and cell survival. Hence, genetic alterations in tyrosine kinase receptors may result in carcinogenesis and cancer development [3]. The finding and enhancement of tyrosine kinase inhibitors targeting tyrosine kinase receptors (TKRs) have been a significant milestone in expanding our understanding of tumor physiopathology and in developing cancer treatments based on molecular changes in numerous tumor types [4]. One of the most prominent oncogenic kinases is epidermal growth factor receptor (EGFR), which is overexpressed in a multiplicity of human cancers, including breast, colorectal, lung, prostate, ovary and pancreatic cancer [5]. Resistance to radiation, hormone therapy, and cytotoxic medications led to poor treatment outcomes. It led to an opportunity for anti-EGFR drug recommendations because of their superior safety and efficacy compared to standard chemotherapy [6]. As a result, the discovery of novel synthesized anti-neoplastic drugs or structural alterations of already recognized molecular cores has offered a rational approach to cancer therapy by inhibiting tyrosine kinase activity [7].

Many heterocyclic compounds are important to medical chemistry due to their exceptional and diverse pharmacological properties [8]. The heterocyclic containing a pyrazole core has numerous pharmacological effects such as antibacterial, antiviral, antifungal, anti-inflammatory, and anti-tumour, among other clinical applications [9]. Molecular docking has become one of the most often utilized approaches in Ligand Based Drug Design (LBDD) due to its ability to accurately anticipate small-molecule ligands' conformation within the desired target binding sites. [10]. As illustrated in figure (2). Molecular docking has become a necessity for drug discovery. Molecular docking methods provide quantitative estimates of binding energies and rank docked molecules based on the binding affinity of ligand-receptor complexes [11]. Our research revealed that new phenyldiazenyl)-pyrazol schiff base derivatives compounds could potentially be potent agents. To develop new EGFR inhibitors, our team concentrated on synthesizing 1,2-pyrazole-based compounds as the pharmacophore core. (A549) lung cancer cell line was used to explore anticancer effects for the compounds (3a–e). Also predicted in silico were the inhibition of EGFR tyrosine kinase and the pharmacokinetics of the investigated compounds.

Materials and Methods

All chemicals were purchased from Sigma Aldrich, USA and hyper-chem, Hangxing RD., Hangzhou, China. Simultaneously,

the melting point was measured by using the method of the capillary tube on an instrument of electric melting point by England Stuart Company, 1H NMR and ^{13}C NMR instruments of (300 and 400 MHz) and (75 and 100) MHz, respectively, using Bruker/ Aligent by USA Company were done in Iran/ university of Tehran, and FT-IR Shimazu 8400s by Japan was done at the College of Pharmacy-Mustansiriyah University

Chemical synthesis

Several novel phenyldiazenyl)-pyrazol schiff base derivatives were synthesized using the following procedures (Scheme1).

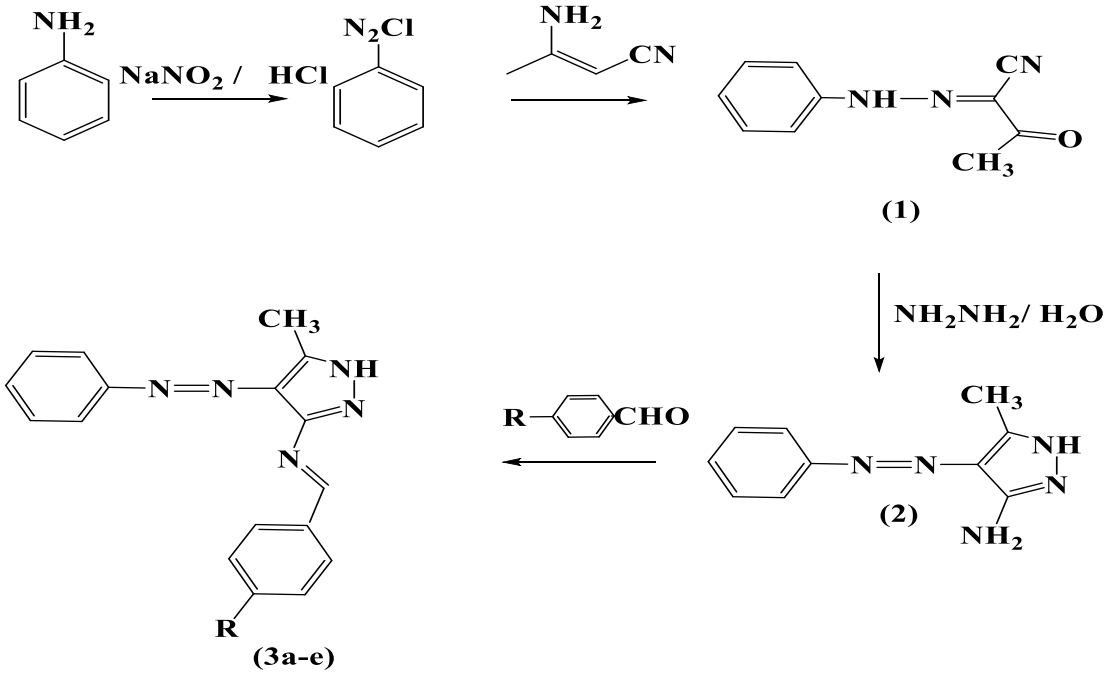

R = (a) $N(CH_3)_2$, (b) NO_2, (c) Cl, (d) CH_3, (e) OCH_3

Synthesis of the 2-oxo-N phenylpropanehydrazonoyl cyanide (1)

In a 100 mL beaker, a solution of aniline (1) (0.186 g, 2 mmol) in concentrated HCl (3 mL) and 2 ml H_2O cooled inside an ice bath and then diazotized with the $NaNO_2$ solution (0.138 g, 2 mmol in 5 mL H_2O) at 0-5℃ added drop wisely. Slowly, the cold diazonium solution was added to a well-stirred solution of 3-aminocrotononitrile (0.164 g, 2 mmol) dissolved in (20 mL) of ethanol containing sodium acetate (2 mmol,1.64 g). Two hours were used for stirring the reaction mixture. The precipitate was filtered and washed with deionized water until litmus paper was neutral. The solid result was collected and recrystallized from ethanol to provide the corresponding hydrazone compounds [12].

Synthesis of the 5-methyl-4-(phenyldiazenyl)-1H-pyrazol-3-amine (2)

Compound 1 (0.37 g, 2 mmol) was dissolved in 20 mL of 1,4 dioxane in a 100 mL round-bottom flask; then, 3 drops of 98% hydrazine hydrate (2 mmol) were added. The mixture was refluxed for 4 hours before being cooled at room temperature. The solid result was filtered, dried, and recrystallized from a

DMF/ethanol combination to produce compound 2[13&14].

General Procedure for the synthesis of the N, N-dimethyl-4-((1E)-((5-methyl-4-(phenyldiazenyl)-1H-pyrazol-3-yl)imino)methyl)aniline (3a-e)

In a 100 mL round bottom flask, compound (2) *5-methyl-4-(phenyldiazenyl)-1H-pyrazole-3-amine* (2 mmol,0.5 g) and different benzaldehyde derivatives (2 mmol) dissolved in a mixture of pyridine (20 mL) and DMF (10 mL) were refluxed for 12 hours. Over the night, the reaction mixture was allowed to stand at room temperature. The separated solid product was filtered, dried, and recrystallized from a mixture of ethanol/benzene to give a distinct colour spectrum ranging from pale yellow to orange crystal [15].

2-oxo-N-phenylpropanehydrazonoyl cyanide (1)

Yellow crystals, Yield, 83%, mp: 166-168, FTIR *v*max (KBr): 3292.64 cm^{-1} (NH), 3014.71cm^{-1} (aromatic C-H), 2979.00cm^{-1} (CH_3), 2214.22 cm^{-1} (CN), 1662.27cm^{-1}(C=O), 1602.01cm^{-1} (C=N), 1538.75cm^{-1} (aromatic C=C); ^{1}H NMR (300 MHz, *DMSO-d6*) δ ppm: 2.17 (3H, s, CH_3), 7.16 – 7.39 (5H, m, Ar-H), 11.31 (1H, s, NH); ^{13}C NMR (75 MHz, *DMSO-d6*) δ ppm: 25.04 (CH_3), 114.07– 129.90 (5CH of aromatic ring), 142.38 (1C of aromatic ring), 111.40 (C=N), 116.68(CN), 193.13 (C=O).

5-methyl-4-(phenyldiazenyl)-1H-pyrazol-3-amine (2)

Brown powder, Yield, 85%, mp: 196-198, FTIR *v*max (KBr): 3441.52&3300.12 cm^{-1}(NH_2), 3180.83 cm^{-1} (NH), 3058.49cm^{-1} (aromatic C-H), 2953.73cm^{-1} (CH_3), 1601.87cm^{-1} (C=N of Pyrazole ring), 1584.31cm^{-1}(aromatic C=C), 1493.55cm^{-1}(N=N); ^{1}H NMR (300 MHz, *DMSO-d6*) δ ppm: 2.41 (3H, s, CH_3), 7.29 (2H, s, NH_2), 7.31 – 7.71 (5H, m, Ar-H), 11.74 (1H, s, NH); ^{13}C NMR (75 MHz, *DMSO-d6*) δ ppm: 11.02 (CH_3), 90.17 (C=C of Pyrazole ring), 125.45-129.46 (5CH of aromatic ring), 129.39 (1C of aromatic ring), 146.55 (C-NH of Pyrazole ring), 153.57 (C=N of Pyrazole ring).

N,N-dimethyl-4-((1E)-((5-methyl-4-(phenyldiazenyl)-1H-pyrazol-3-yl)imino)methyl)aniline (3a)

Brown crystals, Yield, 70% mp: 124-126, FTIR *v*max (KBr): 3191.69 cm^{-1} (NH), 3060.00cm^{-1} (aromatic C-H), 2962.12cm^{-1} (CH_3), 1659.64cm^{-1} (C=N of Schiff base), 1589.07cm^{-1}(C=N of Pyrazole ring),1523.98cm^{-1}(aromatic C=C), 1479.11cm^{-1}(N=N),1313.50cm^{-1} (C-N(CH_3)$_2$);^{1}H NMR (400 MHz, DMSO) δ ppm: 2.31 (3H, s, CH3), 3.02 (6H, s, N(CH_3)$_2$), 6.83– 7.42 (9H, m, Ar-H), 8.87 (1H,s, N=CH), 11.86(1H, s, NH);^{13}C NMR (100 MHz, *DMSO-d6*) δ ppm: 10.65 (CH_3), 56.76(6H,s, N(CH_3)$_2$), 111.53 (C=C of Pyrazole ring), 112.02-128.31 (9CH of aromatic ring), 123.68-154.66 (3C of aromatic ring), 140.75(C-NH of Pyrazole ring),153.55(C=N of Pyrazole ring), 157.86(C=N of Schiff base).

(1E)-N-(5-methyl-4-(phenyldiazenyl)-1H-pyrazol-3-yl)-1-(4-nitrophenyl)methanimine(3b)

Yellowish red crystal, Yield, 66% mp: 170-172, FTIR *v*max (KBr): 3196.47 cm^{-1}(NH), 3063.00cm^{-1} (aromatic C-H), 2954.43cm^{-1} (CH_3), 1656.01cm^{-1} (C=N of Schiff base), 1598.97cm^{-1}(C=N of Pyrazole ring),1571.76cm^{-1}(aromatic C=C),1480.10cm^{-1}(N=N), 1519&1343cm^{-1} (NO_2);^{1}H NMR (300 MHz, *DMSO-d6*) δ ppm: 2.32 (3H, s, CH3), 7.13– 8.34 (9H, m, Ar-H), 8.81 (1H,s, N=CH) 11.90(1H, s, NH);^{13}C NMR (75 MHz, *DMSO-d6*) δ ppm: 9.47 (CH3),115.19 (C=C of Pyrazole ring), 124.73-128.79 (9CH of aromatic ring), 129.44-152.48 (3C of aromatic ring), 141.88 (C-NH of Pyrazole ring), 148.15

(C=N of Pyrazole ring), 157.29 (C=N of Schiff base).

(1E)-1-(4-chlorophenyl)-N-(5-methyl-4-(phenyldiazenyl)-1H-pyrazole-3-yl)methanimine (3c)

yellow crystal, Yield, 60% mp: 192-194, FTIR *v*max (KBr): 3205.14cm-1(NH),3060.06cm-1 (aromatic C-H), 2952.28cm–1 (CH_3), 1662.93cm–1 (C=N of Schiff base), 1588.55cm–1(C=N of Pyrazole ring), 1567.97cm–1(aromatic C=C), 1480.06cm–1(N=N), 815.94cm–1 (C-Cl);^{1}H NMR (300 MHz, *DMSO-d6*) δ ppm: 2.33 (3H, s, CH3), 7.11– 7.45 (9H, m, Ar-H), 8.83 (1H,s, N=CH), 11.90(1H, s, NH); ^{13}C NMR (75 MHz, *DMSO-d6*) δ ppm: 10.38 (CH3),109.90 (C=C of Pyrazole ring), 115.35-131.11 (9CH of aromatic ring), 126.53-142.84 (3C of aromatic ring), 146.96 (C-NH of Pyrazole ring),146.96 (C=N of Pyrazole ring), 152.55 (C=N of Schiff base).

(1E)-N-(5-methyl-4-(phenyldiazenyl)-1H-pyrazol-3-yl)-1-(p-tolyl)methanimine (3d)

orange powder, Yield, 78% mp: 186-188, FTIR *v*max (KBr): 3201.47cm-1(NH),3059.05cm-1 (aromatic C-H), 2955.44cm^{-1} (CH_3), 1661.44cm^{-1} (C=N of Schiff base), 1598.16cm^{-1}(C=N of Pyrazole ring), 1587.74cm^{-1}(aromatic C=C), 1478.72cm^{-1}(N=N), 1088.12cm^{-1} (C-CH3);^{1}H NMR (300 MHz, *DMSO-d6*) δ ppm: 2.39-2.43 (9H, s, CH_3),7.16– 7.42 (9H, m, Ar-H), 8.82 (1H,s, N=CH);11.88(1H,s,NH);^{13}CNMR (75 MHz, *DMSO-d6*) δ ppm: 11.12-20.68 ($2CH_3$),111.19(C=C of Pyrazole ring), 116.95-129.46 (9CH of aromatic ring), 126.63-140.92(3C of aromatic ring), 143.35 (C-NH of Pyrazole ring) 153.56 (C=N of Pyrazole ring), 159.82(C=N of Schiff base).

(1E)-1-(4-methoxyphenyl)-N-(5-methyl-4-(phenyldiazenyl)-1H-pyrazol-3-yl)methanimine (3e)

yellow crystal, Yield, 69% mp: 122-124, FTIR *v*max (KBr): 3210.71cm-1(NH),3063.70cm-1 (aromatic C-H), 2954.01cm^{-1} (CH_3), 1600.89cm^{-1} (C=N of Schiff base), 1570.31cm^{-1}(C=N of Pyrazole ring), 1538.62cm^{-1}(aromatic C=C), 1481.24cm^{-1}(N=N), 1248.23cm^{-1} (C-OCH_3);^{1}H NMR (300 MHz, DMSO) δ ppm: 2.31 (3H, s, CH_3), 2.79 (3H, s, OCH_3),7.12– 7.56 (9H, m, Ar-H),8.97(1H,s,N=CH);11.97(1H,s,NH);^{13}C NMR (75MHz, *DMSO-d6*) δppm: 9.34 (CH_3), 55.66 (OCH_3) 114.83 (C=C of Pyrazole ring), 114.99-129.46 (9CH of aromatic ring), 124.88-142.81(3C of aromatic ring), 144.39 (C-NH of Pyrazole ring) 153.52(C=N of Pyrazole ring), 159.86(C=N of Schiff base).

ADME Procedure

Using the Swiss ADME server, all ligands' physicochemical and pharmacokinetic characteristics were determined (3a-e). Utilizing Swiss ADME, the Chem. Sketch (v.12) chemical structure of proposed compounds was converted to SMILE name [16].

Docking Studies

Molecular docking studies are a valuable technique for developing new drugs, as they permit ligand-receptor interaction and biological activity prediction. CCDCGOLD Suite (version 5.7.1) incorporates Hermes visualizer software (version 1.10.1) for the display of receptors, ligands, interaction type (short contact, H-bond), bond length, and active site computation [17].

Receptor and ligands Preparation

(EGFR) epidermal growth factor tyrosine kinase structure (PDB ID: 1M17) [18] retrieved from the protein data bank (PDB). Crystal structure of the protein

requires two steps: preserving water molecules through interaction sites and removing others, and introducing hydrogen atoms to establish the amino acid residues'; tautomeric state of the amino acid residues and proper ionization. CheBio3D (19.1) and the MM2 force field were used to minimize the energy of synthesized compounds.

Protocol for Molecular Docking

GOLD Suite (HERMES) structure visualization software was used to set up the receptors for the docking procedure [19]. Proteins reference ligand was used to determine the active site's radius (10 Å). ChemScore kinase has been used as a template for configuration. The scoring function consisted of ChemPiecewise linear potential (CHEMPLP). During the docking process, the values of all parameters were kept the default, and the evaluation of each solution was based on the CHEMPLP fitness function, as the interaction of the ligation with the protein residues of the tyrosine kinase enzyme. The docking outcomes, such as binding mode, docked posture, and binding free, were utilized.

Cytotoxicity Test

MTT assay was performed to evaluate the cytotoxic efficacy of (3a-e) against the survival of the lung cancer cell line (A549) [20]. This procedure occurred in the College of Pharmacy of Mustansiriyah University in Iraq.

Culture and Maintenance of Cells

ATCC provides lung cancer cell lines (A549). It was kept at Mustansiriyah University's College of Pharmacy in the Tissue Culture Research Center's Cell Bank. (A549) cells were cultivated in RPMI-1640 media complemented with 1% L-Glutamine, 10% FBS and 1% Penicillin Streptomycin-Amphotericin B 100X as an antiseptic.

The Half Maximal Inhibitory Concentration

Value Determination by the *in vitro* MTT test, the IC_{50} is the concentration of the investigated compounds (3a-e) required to cause a 50% reduction in cell viability. The IC_{50} values for compounds (3a-e) were evaluated using the in vitro MTT assay 72 hours after these compounds were administered to the cells. To calculate the IC_{50}, plot the corrected absorbance at 560-600 nm (absorbance minus complete media) against the test compound concentration (absorbance minus complete media) against the test compound concentration. In a triplicate, [Inhibition Rate%= (A-B/A) * 100] was used to compute the percent inhibition rate (percentage of cytotoxicity).

Statistical analysis

GraphPad Prism and nonlinear curve fitting software was used to statistically analyze the MTT assay data and IC_{50} values of investigated compounds (3a-e) on lung cancer cell lines. To compare all groups on the same MTT plate, a one-way ANOVA with the Tukey test was performed, and the results were analyzed by (prism and software).

Result interpretation for ADME

Swiss ADME server assessed the outcomes of the ADME properties of the final synthesized compounds to identify the most effective drug candidate(s) and the safest and to exclude compounds that may fail in further drug development stages due to incorrect ADME properties. [21]. All synthesized compounds' Pharmacokinetic parameters (absorption, distribution, metabolism, and excretion) were evaluated. Topological polar surface area (TPSA) was calculated since it is crucial in determining medication bioavailability. [22]. All synthesized compounds' results showed that TPSA is below 140. Hence, it is assumed that passively absorbed

compounds with a TPSA < 140 Ao have great oral bioavailability. The bioavailability for all synthesized ligands was 0.55, indicating that all ligands entered the systemic circulation, as shown in table (1). Following oral administration, the GI absorption score represents a chemical's intestinal absorption degree. If the result was high, absorption might be favorable. In our research, the GI absorption of all produced compounds, except compound (3b), was high, as we would anticipate.

Table (1): The result of ADME for the final derivatives

Comp name:	Molecular formula	M.wt	M log p	H-bond donor	H-bond acceptor	TPSA	GI-Solubility
3a	$C_{19}H_{20}N_6$	332.4	3.03	1	4	69.00 A	high
3b	$C_{17}H_{14}N_6O_2$	334.3	2.12	1	6	111.5 A	low
3c	$C_{17}H_{14}ClN_5$	323.8	3.61	1	4	65.76 A	high
3d	$C_{18}H_{17}N_5$	303.4	3.34	1	4	65.76 A	high
3e	$C_{18}H_{17}N_5O$	319.4	2.80	1	5	74.99 A	high

Interpretation of docking results

The GOLD refers to a "genetic approach for docking flexible ligands into protein binding sites" [23]. GOLD exhibited excellent posture prediction rendering and virtual screening results and undergo extensive validation [24]. This section of the GOLD Suite includes GoldMine, Mercury, Isostar, Hermes, and Conquest. The GOLD Suite program docked all created compounds successfully (3a-e). It is essential to decrease the energy of ligands and proteins to repair distorted geometries via the rearrangement of molecules to eliminate internal limitations. Subsequently, minimizing the energy, the geometry is restored to demonstrate that the smallest amount of energy has been obtained. To anticipate the binding energies and the selectivity of the ligands for the target, we assessed the interactions between the target and our ligands (3a-e) in the model complexes. We observed the fitness function ability of this complex by all of the desired compounds. Binding affinity of EGFR receptors and compounds (3a-e) were ranked based on their PLP fitness average in the complex formation at the active sites. The PLP fitness ranges of the docked compounds on the target were found (68.70 to 76.14) with their amino acid interactions, as shown in table (2) and figures (4 to 9). In our work, the synthesized ligand (3a) gave promising

docking results with EGFR tyrosine kinase showed the best docking on PLP fitness (76.14). In contrast, compound 3b had PLP fitness (73.32) closely related to the Erlotinib score PLP fitness (74.80). While compounds (3c, 3d and 3e) had PLP fitness (70.34&72.64 &68.70), respectively. The correlation between our docking analysis and the experimental results is finally compatible.3D structural picture of Hydrogen bond (green color) and short contact interaction (red color) profiles of all compounds binding with EGFR (code of PDB: 1M17). Compounds are administered in a stick-and-ball format; wherever amino acids are administered as capped sticks as shown in figures (4 to 9).

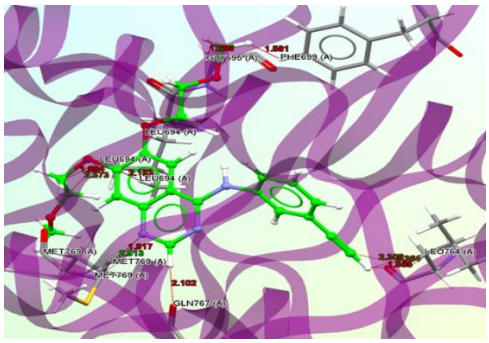

Figure (4): 3D structural picture of Erlotinib binding with EGFR (code of PDB: 1M17).

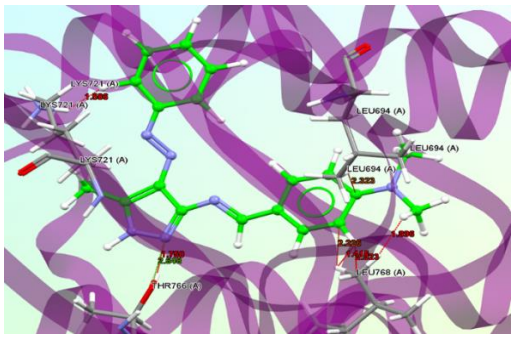

Figure (5): 3D structural picture of 3a binding with EGFR (code of PDB: 1M17)

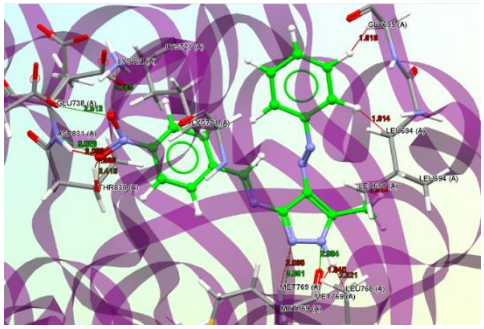

Figure (6): 3D structural picture of 3b binding with EGFR (code of PDB: 1M17).

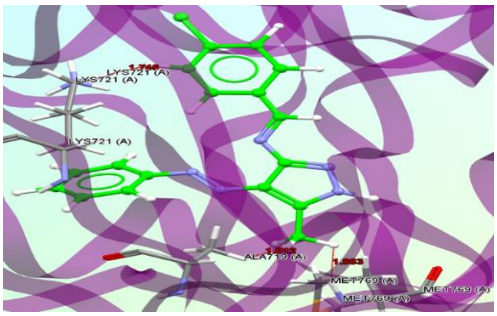

Figure (7): 3D structural picture of 3c binding with EGFR (code of PDB: 1M17).

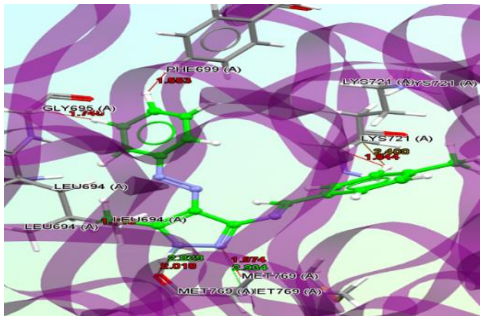

Figure (8): 3D structural picture of 3d binding EGFR (code of PDB: 1M17).

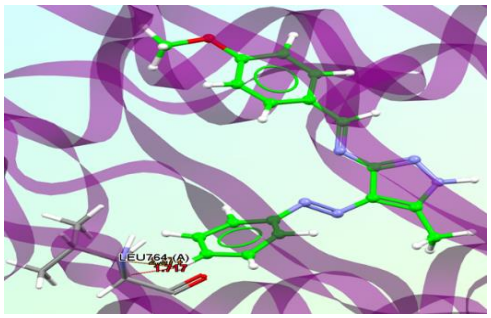

Figure (9): 3D structural picture of 3e binding EGFR (code of PDB: 1M17).

Table (2): The binding energies of our final compounds.

Protein data bank	Compounds	Binding g Energy (PLP Fitness)	Amino Acids Included in H-Bond and Short contact interactions
Epidermal Growth factor (EGFR) Tyrosine kinase code: (1M17)	3a	76.14	THR766 LYS 721 THR 766 LEU 768 (4) LEU 694
	3b	73.32	MET 769 (2), ASP 831 THR 830 (2), MET 769 GLY 695, LEU 768 (2) LEU 694 (2), ASP 831 THE 830, GLU 738 LYS 721
	3c	70.34	MET 769 ALA 719 LYS 721
	3d	72.46	LYS 721 (2) PHE 699 GLY 695 LEU 694 MET 769 (4)
	3e	68.70	ALA 719 (2) MET 769 LYS 721
	Erlotinib	70.80	MET 769 GLN 767 LEU 694 (3) GLY 695 PHE 699 LEU 764 (3)

Interpretation of antiproliferative Effects on a Breast Cancer Cell Line

The antiproliferative effect of the manufactured compounds (3a-e) was demonstrated by MTT assay, as shown in table (3). Compounds (3a and 3b) had the most potent antiproliferative effect on the A549 cell line, with IC_{50} values of (17.37 and 25.82) µM, respectively. Compound 3a is approximately 1.4 times more active

than Erlotinib. In contrast, compound 3b is closely related to the reference drug, indicating that compound (3a) requires a lower concentration to inhibit the growth of cancerous A549 cells than Erlotinib. In contrast, the IC_{50} values for compounds 3c, 3d, and 3e were 47.48, 45.56, and 33.05 µM, respectively. Figure (10) illustrates the dose-response curve for the IC_{50} value of Erlotinib on A549, whereas figures (11–15) depict dose-response curves for the IC_{50} value of our powerful drugs.

Table (3): Indicate the IC_{50} of final compounds produced and Erlotinib.

Type of the cell	Compound 3a	Compound 3b	Compound 3c	Compound 3d	Compound 3e	Erlotinib.
A459	17.37	25.82	47.48	45.56	33.03	25.06

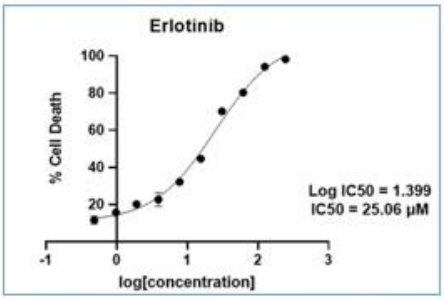

Figure (10): Dose-response curve (IC_{50})of Erlotinib on A549

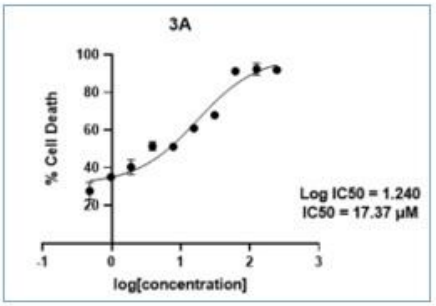

Figure (11): Dose-response curve the (IC_{50})of the compound (3a) on A549

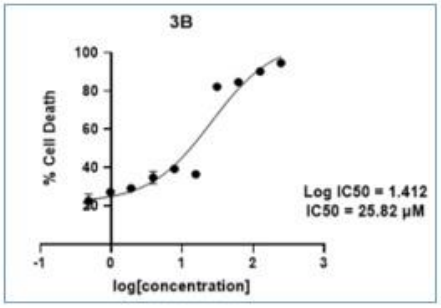

Figure (12): Dose-response curve (IC_{50}) compound (3b) on A549.

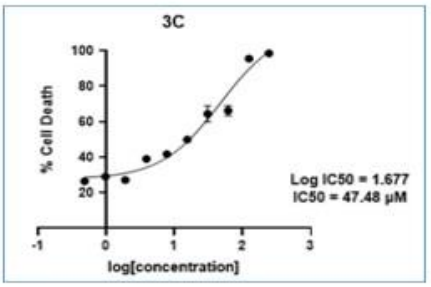

Figure (13): Dose-response curve of (IC_{50})of the compound(3c)onA549

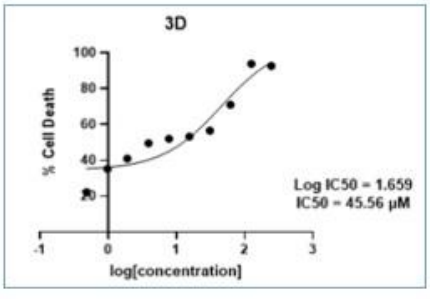

Figure (14): Dose-response curve(IC_{50}) of the compound (3d) on A549

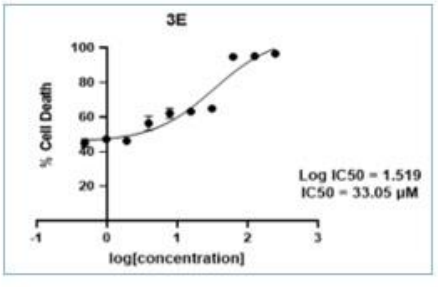

Figure(15):Doseresponsecurve(IC_{50}) of the compound (3e) on A549

Result and Discussion

The target compounds (3a-e) were effectively synthesized using their intermediates. In this work, we predict the synthesis of a new phenyldiazenyl)-pyrazol schiff base derivatives. The target compounds were obtained by reacting azo dye with 3-aminocrotononitrile to form compound 1. The compound 1 was confirmed by their FT-IR spectroscopy. the FT-IR spectrum of compound (1) shows appearance of the characteristic absorption bands for υ NH stretching at 3308.35 cm^{-1}, υ CN stretching at 2213.76 cm^{-1}, υ C=O stretching at 1662.27^{-1}, υ C=N stretching at region 1602.01cm^{-1} and disappearance of strong band of both the υ NH_2 stretching at region 3434.21 and 3342.33cm^{-1} of 3-aminobut-2-enenitrile.

^{1}H-NMR results have shown singlet for NH protons at 11.31 (δ, ppm).and disappearance signal of NH_2 proton of 3-aminobut-2-enenitrile at 6.81 (δ, ppm).

Moreover, ^{13}C-NMR results have shown the disappearance of C-NH_2 of 3-aminobut-2-enenitrile at 163.68 δ and is replaced by C=O group at 193.13 δ.

The compound (1) was interact with hydrazine hydrate to form compound 2. Compound 2 was confirmed by its FT-IR spectroscopy. The FT-IR spectrum of compound (2) indicated the formation of the characteristic absorption band of υ NH_2 at 3441.52 and 3300.12 cm-^{1}, υ NH of the pyrazole ring at 3180.83 cm^{-1} and the disappearance of the υ C=O and υ CN bands of the previous compound at 1662.27cm^{-1} and 2213.76 cm^{-1}, respectively.

^{1}H-NMR results have shown singlet for NH_2 and NH proton at 7.29 (δ, ppm) and 11.74(δ, ppm), respectively, as shown in figure (16).

^{13}C-NMR peaks for compound 2 indicated that the Pyrazole ring's C=C, C-NH and C=N are at 90.17 δ,146.55 δ and 153.57 δ respectively. In addition, the CN and C=O bands of the previous compound disappear at 116.68 δ and 193.13 δ, respectively.

Compound (2) was interact with different benzaldehyde derivatives that dissolved in a mixture of DMF/Pyridine to form the compounds (3a-e). The structure of compounds 3(a-e) was confirmed by their FT-IR spectroscopy. FT-IR spectrum of compound 3(a-e) showed the appearance of the characteristic absorption band of υ C=N stretching of imine at (1659.64, 1656.01, 1662.93, 1661.64 and 1660.89 cm^{-1}).

^{1}H-NMR result for compounds (3a-e) revealed singlets for the N=CH proton of Schiff bases at 8.87, 8.81, 8.83, 8.82 and 8.97 δ, ppm, respectively.

^{13}C-NMR peaks for compounds (3a-e) indicated C=N of Schiff base at 157.86, 157.29, 152.55, 159.82 and 159.86 δ, respectively.

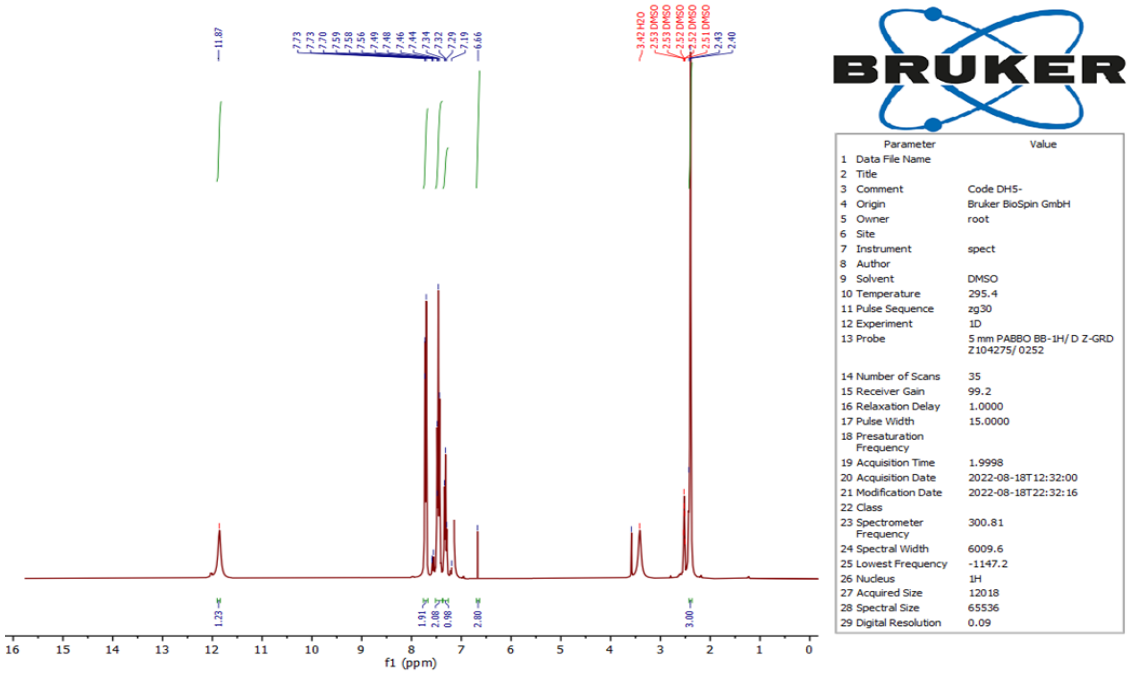

Figure (16): ^{1}H NMR spectrum of compound 2

Conclusion

The antiproliferative evaluation *in vitro* reveals that several compounds containing phenyldiazenyl)-pyrazol schiff base derivatives give excellent antiproliferative activity against lung cancer. The best compound (3a) showed a high antiproliferative against the A549 lung cancer cell line. In addition, compound 3b exhibited superior antiproliferative activity against the EGFR tyrosine kinase (A549) cell line comparable to Erlotinib. Furthermore, the ADME study revealed that each produced compound satisfied the Lipinski criterion.

References:

1- Saba T. Recent advancement in cancer detection using machine learning: Systematic survey of decades, comparisons and challenges. Journal of Infection and Public Health. 2020 Sep 1;13(9):1274-1289.

2- Mattiuzzi C, Lippi G. Current cancer epidemiology. Journal of epidemiology and global health. 2019 Dec;9(4):217.

3- Esteban-Villarrubia J, Soto-Castillo JJ, Pozas J, San Román-Gil M, Orejana-Martín I, Torres-Jiménez J, Carrato A, Alonso-Gordoa T, Molina-Cerrillo J. Tyrosine kinase receptors in oncology. International journal of molecular sciences. 2020 Nov 12;21(22):8529.

4- Saraon P, Pathmanathan S, Snider J, Lyakisheva A, Wong V, Stagljar I. Receptor tyrosine kinases and cancer: oncogenic mechanisms and therapeutic approaches. Oncogene. 2021 Jun 17;40(24):4079-4093.

5- Scaltriti M, Baselga J. The epidermal growth factor receptor pathway: a model for targeted therapy. Clinical cancer research. 2006 Sep 15;12(18):5268-5272.

6- Vasan N, Baselga J, Hyman DM. A view on drug resistance in cancer. Nature. 2019 Nov 14;575(7782):299-309.

7- Ibrahim NW, Mahdi M, Raauf AM. Design, Molecular Docking, Synthesis and Evaluation of New Isatin Derivatives Bearing Pyridine Moiety as Potential Tyrosine Kinase Inhibitors. Egyptian Journal of Chemistry. 2022 Feb 1;65(2):9-18.

8- Alawad KM, Mahdi MF, Raauf AM. Molecular Docking, Synthesis, Characterization and Adme Studies of Some New Five-Member Ring Heterocyclic Compounds with in Vitro Antiproliferative Evaluation. Journal of Hunan University (Natural Science Edition). 2021 Sep;48(9).

9- Karrouchi K, Radi S, Ramli Y, Taoufik J, Mabkhot YN, Al-Aizari FA, et al. Synthesis and pharmacological activities of pyrazole derivatives: A review. Molecules. 2018;23(1):134.

10- Ferreira LG, Dos Santos RN, Oliva G, Andricopulo AD. Molecular docking and structure-based drug design strategies. Molecules. 2015 Jul 22;20(7):13384-13421.

11- Fadhil HR, Mahdi MF, Raauf AM. MOLECULAR DOCKING, SYNTHESIS, CHARACTERIZATION AND ANTIPROLIFERATIVE EVALUATION OF PYRAZOLINE DERIVATIVES.

12- Azab ME, Youssef MM, El-Bordany EA. Synthesis and antibacterial Evaluation of novel heterocyclic compounds containing a sulfonamido moiety. Molecules. 2013;18(1):832–844.

13- Saleh MA, Abdel-Megeed MF, Abdo MA, Shokr A-BM. Synthesis of novel 3H-quinazolin-4-ones containing pyrazolinone, pyrazole and pyrimidinone moieties. Molecules. 2003 ;8(4) :363–373.

14- Elnagdi MH, Sallam MM, Fahmy HM, Ibrahim SA, Elias MA. Reactions with the Arylhydrazones of α-Cyanoketones: The Structure of 2-Arylhydrazono-3-ketimino-nitriles. Helvetica Chimica Acta. 1976 Mar 10;59(2):551-7.

15- Metwally MA, Gouda MA, Harmal AN, Khalil AM. 3-Iminobutanenitrile as building block for the synthesis of substituted pyrazolo [1, 5-a] pyrimidines with antitumor and antioxidant activities. International Journal of Modern Organic Chemistry. 2012; 1:96-114

16- Daina, A., O. Michielin, and V. Zoete, SwissADME: a free web tool to evaluate pharmacokinetics, drug-likeness and medicinal chemistry friendliness of small molecules.Scientific reports, 2017. 7(1): p. 1-13.

17- Nawaz, F., et al., 3′- (4- (Benzyloxy) phenyl) -1′- phenyl- 5- (heteroaryl/aryl) - 3, 4- dihydro-1′ H, 2H- [3, 4′- bipyrazole] - 2- carboxamides as EGFR kinase inhibitors: Synthesis, anticancer Evaluation, and molecular docking studies. Archivder Pharmazie, 2020. 353(4): p. 1900262.

18- Park, J.H., et al., Erlotinib binds both inactive and active conformations of the EGFR tyrosine kinase domain. Biochemical Journal, 2012. 448(Pt 3): p.417.

19- Yousif OA, Mahdi MF, Raauf AM. Design, synthesis, preliminary pharmacological evaluation, molecular docking and ADME studies of some new pyrazoline, isoxazoline and pyrimidine derivatives bearing nabumetone moiety targeting cyclooxygenase enzyme. Journal of Contemporary Medical Sciences. 2019 Jan;5(1):41-50.

20- Zhang L, Chen Q, Hou G, Zhao W, Hou Y. Hydroxyl-substituted double Schiff-base condensed 4-piperidone/cyclohexanones as potential anticancer agents with biological Evaluation. Journal of enzyme inhibition and medicinal chemistry. 2019 Jan 1;34(1):264-71.

21- Adnan, A.M.A., M.F. Mahdi, and A. Kareem Khan, Design, Synthesis, and Acute Anti-inflammatory Assessment of New 2-methyl Benzoimidazole Derivatives Having 4- Thiazolidinone Nucleus. Al-Mustansiriyah Journal of Pharmaceutical Sciences (AJPS), 2019. 19(4): p. 151-160.

22- Wabdan AK, Mahdi MF, Khan AK. Molecular Docking, Synthesis and ADME Studies of New Pyrazoline Derivatives as Potential Anticancer Agents. Egyptian Journal of Chemistry. 2021 Aug 1;64(8):4311-4322.

23- Sahoo RN, Pattanaik S, Pattnaik G, Mallick S, Mohapatra R. Review on the use of Molecular Docking as the First Line Tool in Drug Discovery and Development. Indian Journal of Pharmaceutical Sciences. 2022 Oct 31;84(5):1334-1337.

24- Shaikh N, Linthoi RK, Swamy KV, Karthikeyan M, Vyas R. Comprehensive molecular docking and dynamic simulations for drug repurposing of clinical drugs against multiple cancer kinase targets. Journal of Biomolecular Structure and Dynamics. 2022 Sep 14:1-9.